Supporting Information

Mimicking microbial rhodopsin isomerization in a single crystal

Alireza Ghanbarpour, Muath Nairat, Meisam Nosrati, Elizabeth M. Santos, Chrysoula Vasileiou, Marcos Dantus, Babak Borhan*, James. H. Geiger*

Table of Contents

A. Materials and Methods

All-*trans* retinal, 13-*cis* retinal, and other chemicals used in this study were purchased from Sigma Aldrich unless otherwise specified. A BioLogic DuoFlow (BioRad) chromatography instrument was used for protein purifications. Source Q and Fast Q anion exchange resins were purchased from GE Health Care. An Ultrasonic Homogenizer from Biologics, Inc was used for sonication of the samples.

B. DNA and Protein Purification

Table S1. PCR steps.

PCR program		
1x	94 °C	3 min
	94 °C	20 sec
20x	temperature 3-5 °C lower than primer melting temperature	50 sec
	72° C	4 min 30 sec
1x	72 °C	10 min
1x	10 ° C	5 min

Table S2. PCR protocol.

Template (DNA plasmid)	70 ng (x µl)
Primer forward	20 pmol (y µl)
Primer reverse	20 pmol (z µl)
dNTP	1 µl
10X pfu buffer	5 µl
Pfu Turbo (DNA polymerase)	1 µl
DI water	43-(x+y+z) µl

C. List of primers:

The hCRABPII-pET17b plasmid previously described[1] was employed for mutagenesis.

L121W
Forward: 5'- GAACTGATCTGGACCATGACG-3'
Reverse: 5'-CGTCATGGTCCAGATCAGTTC-3'

L121E
Forward: 5'- GAACTGATCGAAACCATGACG-3'
Reverse: 5'-CGTCATGGTTTCGATCAGTTC-3'

L121Y
Forward: 5'- GAACTGATCTACACCATGACG-3'
Reverse: 5'- CGTCATGGTGTAGATCAGTTC-3'

L121Q
Forward: 5'- GAACTGATCCAGACCATGACG-3'
Reverse: 5'- CGTCATGGTCTGGATCAGTTC-3'

P39Y
Forward: 5'- GCAGCGTCCAAGTATGCAGTGG -3'
Reverse: 5'- CCACTGCATACTTGGACGCTGC - 3'

P39Q
Forward: 5'- GCAGCGTCCAAGCAAGCAGTGG-3'
Reverse: 5'- CCACTGCTTGCTTGGACGCTGC-3'

A32Y
Forward: 5'-GAGGAAGATTTATGTGGCTGC-3'
Reverse: 5'-GCAGCCACATAAATCTTCCTC-3

T54V
Forward: 5'-CTACATCAAAGTCTCCACCACCGTGCG -3'
Reverse: 5'- CGCACGGTGGTGGAGACTTTGATGTAG -3'

R111K
Forward: 5'-CCCAAGACCTCGTGGACCAAAGAACTGACCAACGATGGG-3'
Reverse: 5'-CCCATCGTTGGTCAGTTCTTTGGTCCACGAGGTCTTGGG-3'

R132Q: Y134F
Forward: 5'- GTTGTGTGCACCCAGGTCTTCGTCCG-3'
Reverse: 5'-CGGACGAAGACCTGGGTGCACACAAC-3'

R59Y
Forward: 5'- CCTCCACCACCGTGTACACCACAGAG -3'
Reverse: 5'- CTCTGTGGTGTACACGGTGGTGGAGG -3'

D. Transformation of PCR product

5 µL of PCR product was added to DH5α competent cells (50 µL) thawed on ice. The sample was kept 30 minutes in ice. After heat-shock at 42℃ for 45 seconds, 450 µL of LB was added to the sample. The sample and agar plate containing ampicillin (100 µg/mL) were incubated at 37℃ for 30 minutes. Then 100 µL of the solution were spread on LB agar plate and incubated at 37℃

overnight. The PCR product was purified using Promega DNA purification Kit.

E. Expression of CRABPII variants

The gene was transformed into BL21 (DE3) pLysE *E. coli* competent cells. The same protocol as mentioned for PCR was exploited with the only difference being the addition 100 µg/mL ampicillin and 28 µg/mL chloramphenicol as antibiotics. To inoculate 1 L of LB with ampicillin (100 µg/mL) and chloramphenicol (28 µg/mL), a single colony was used. After the cell culture was grown at 37 ℃ while shaking for 8-10 h, (OD~0.8-0.9) the overexpression was started by adding 1 mL of 1M IPTG solution into 1 L cell culture (overall concentration 1.0 mM of IPTG). The solution was shaken at 19 ℃ for 36 hours.[1, 2]

F. Protein Isolation and Purification

By centrifuging for 20 min at 5,000 rpm (4 ℃) the cells were collected. The supernatant was discarded and the cells were resuspended in 60 mL of Tris buffer (10 mM Tris.HCl, pH=8.0). Then ultrasonication was used to lyse the cells (Power 60%, 1 min x 3), and the sonicated mixture centrifuged at 16 ℃ (10,000 rpm, 20 min).

Purification by ion exchange chromatography using Q SepharoseTM, Fast Flow resin was next performed at 4 ℃. The protein was bound to the column by gravity flow, the column washed with 50 mL of 10 mM Tris.HCl buffer (pH=8.0). The bound protein was then eluted with 50 mL of 150 mM NaCl, 10 mM Tris.HCl pH = 8.0, the pure fractions desalted using EMD Millipore centriprep centrifugal units (cutoffs:10 KDa) with 10 mM Tris.HCl pH=8.0 buffer, three times, and loaded on a second anion exchange column (15Q, GE Health Sciences, BioLogic DuoFlow system).[2] The Source Q program, the same as mentioned previously,[1] was used for the purification.

G. UV-vis measurements

UV-vis spectroscopy was performed using a Cary 300 and Cary 100 Bio Win UV UV-Vis spectrophotometer (Varian Instruments). The samples were prepared in phosphate buffer purchased from Sigma Aldrich. The concentration of retinal was kept at 0.5 equivalent of the protein concentration in all experiments. The PSB has absorptions corresponding to λ_{max} > 450 nm, while deprotonated imine peaks (SB) appear at λ_{max} ~370 nm.

All-*trans* retinal extinction coefficient in ethanol is 48,000 $M^{-1}cm^{-1}$ at 368 nm and 13-*cis* retinal extinction coefficient in ethanol is 38,770 $M^{-1}cm^{-1}$ at 363 nm as reported.[3]

Protein extinction coefficients for different variants were calculated using Gill and Hippel method.[4]

M1 ε_{280nm}= 22,400 $M^{-1}cm^{-1}$

M1-L121E ε_{280nm}= 22,283 $M^{-1}cm^{-1}$

M1-L121Q ε_{280nm}= 20,293 $M^{-1}cm^{-1}$

M1-L121E:P39Q ε_{280nm}= 16,776 $M^{-1}cm^{-1}$

M1-L121E:A32Y ε_{280nm}= 24,500 $M^{-1}cm^{-1}$

H. pK_a determination of mutants

The pK_a was determined by titration (absorbance vs. pH) and was fitted by the protocol previously described.[2] The following equation was used for fitting the data and calculating pK_a by employing KaleidaGraph: $\Delta A = \Delta A_0 / (1+10^{[pH-pKa]})$

I. Irradiation of protein/retinal complexes in solution

An Oriel Illuminator (Model 66142, Oriel Instruments) attached to a power supply [Model 668820, Oriel Instruments, 500 W Mercury (Xenon) lamp] was employed for the light irradiation of samples. A combination of two filters was utilized for all light irradiations. A glass filter (6 mm thickness) was utilized to filter UV light below 320 nm. The second filter for UV irradiations was a U-360 (UV) 2" square band-pass filter [center wavelength (CWL) = 360 nm, full width at half-maximum height (FWHM)= 45 nm, purchased from Edmund Optics, For visible light green light irradiations, a Y-50 2" square long-pass filter (cut-off position = 500 ± 6 nm, purchased from Edmund Optics) was used. The third filter was a 440±20 nm UV-VIS Bandpass Filter purchased from Edmund Optics for blue irradiation.[5]

J. Protein crystallization

The proteins were concentrated to ~ 20-25 mg/ml using EMD Millipore centriprep centrifugal units (cutoffs: 10 KDa) and ~4 equiv. of ligands (all-*trans* retinal or 13-*cis* retinal) were added in the dark. The vapor diffusion method was used for crystallization using 24 well plates in the dark (purchased from Hampton Research) with 1 ml solution in the reservoir. **M1**-L121E, **M1**-L121Q bound with all-*trans* and **M1**-L121E:A32Y bound with 13-*cis* retinal were crystallized under the following conditions: 20% PEG 3350 and 0.1 M DL-malic acid (titrated with NaOH to pH=6.0 and 6.5) at 4° C. For **M1**-L121W, **M1**-L121Y the crystals grew in 20% PEG 3350 and 0.1 M sodium malonate (pH=6.0-6.5) at 4° C. For **M1**-L121E:P39Q, the crystals grew in 20% PEG 3350, 0.1 M bis-tris propane (pH=6.0-6.5), and 0.2 M sodium fluoride at 4° C. All crystals appeared after 1-3 days and were then frozen using liquid nitrogen in a cryogenic buffer containing their mother liquor along with 20% glycerol in the dark. Diffraction data were collected at the Advanced Photon Source (APS) (Argonne National Laboratory IL) LS-CAT, (sector 21-ID-D,F, and G) using either an Eiger 9M, MAR300 or MAR350 detector, and 1.00Å wavelength radiation at 100K. The initial diffraction data were indexed, processed and scaled using the HKL2000[6] software package. The structures were solved by molecular replacement using PHASER[7] in PHENIX [8] and hCRABPII variant (PDB entry 4YFP) as a search model. The initial electron density map was produced using Phaser-MR in PHENIX. Model rebuilding, placement of water molecules etc. were done using COOT[9]. The structures were refined using the PHENIX program package. The chromophore was built using COOT and PHENIX programs to generate restraints.

K. UV-vis measurements for M1/retinal and M1- L121E/retinal complexes

a) M1 bound with all-*trans* retinal.

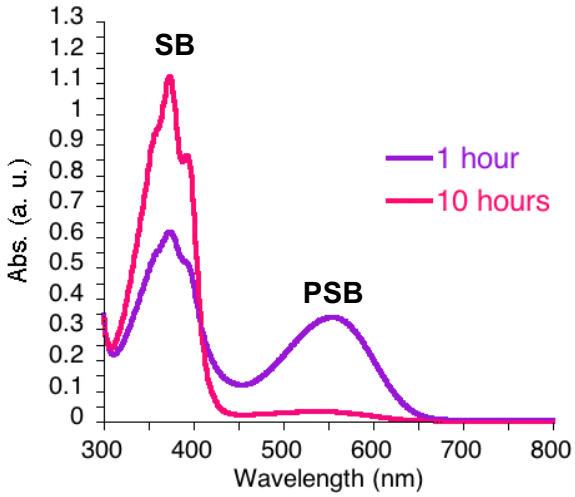

b) M1 bound with 13-*cis* retinal

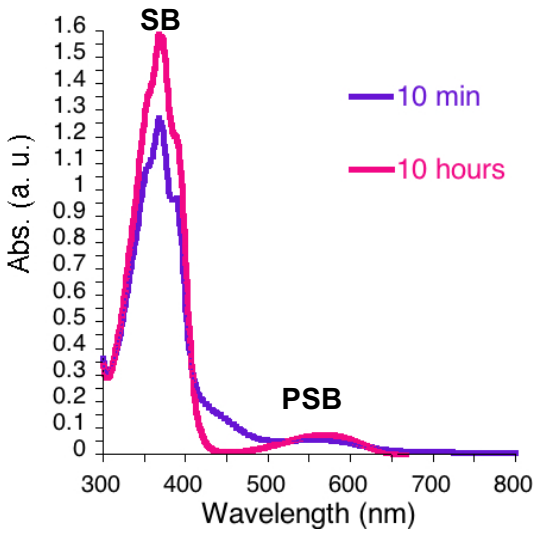

c) M1- L121E- bound with all-*trans* retinal.

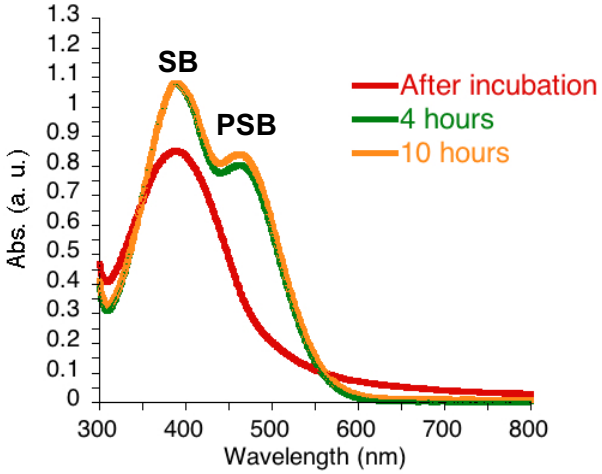

d) M1- L121E- bound with 13-*cis* retinal.

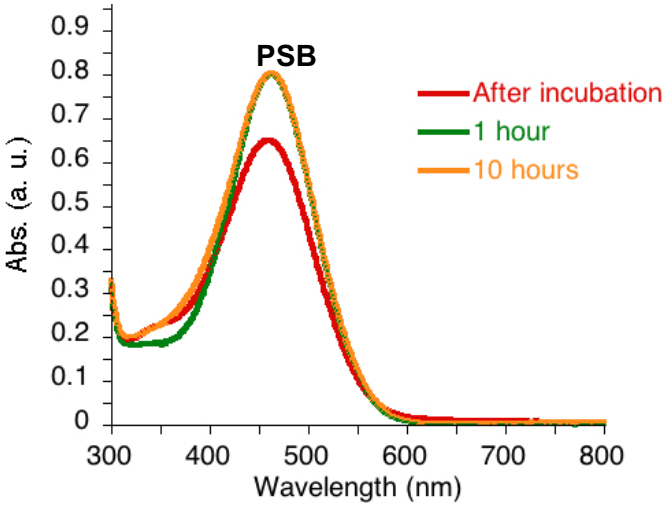

Figure S1. UV-vis spectra of **M1** and **M1**-L121E upon incubation with all-*trans* and 13-*cis* retinal. The SB (Schiff Base, Imine) and PSB (Protonated Schiff Base, Iminium) peaks are highlighted.

L. pK_a determination for M1- L121E/retinal complex

M1-L121E/all-*trans* retinal base titration.

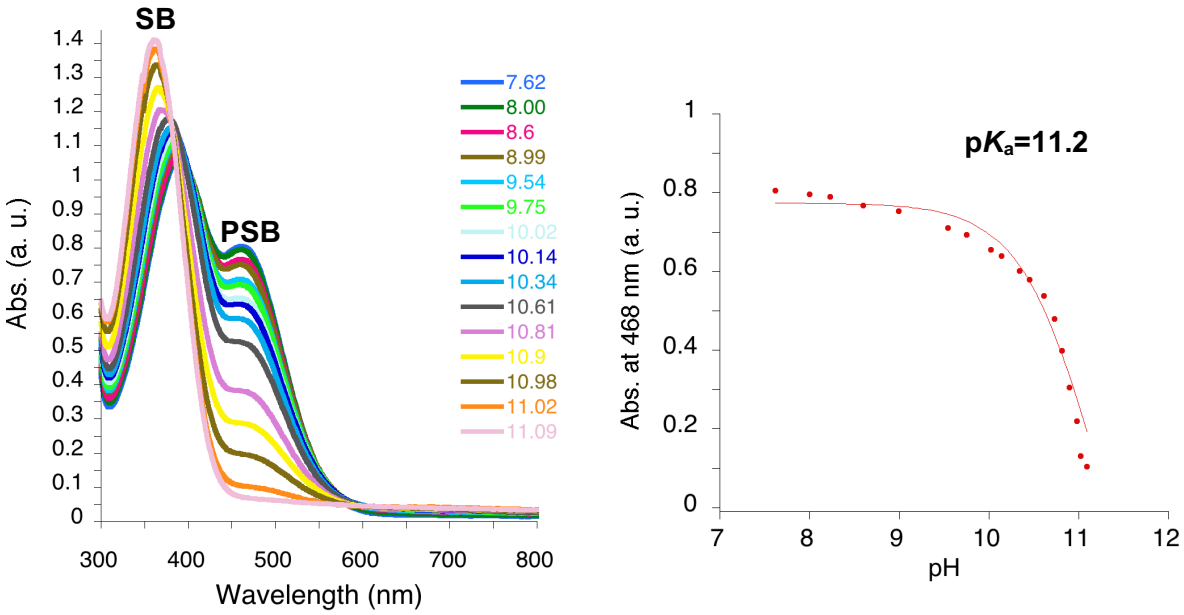

Figure S2. Base titration for **M1**-L121E bound with all-*trans* retinal. Left panel: UV-vis spectra for each mutant; Right panel: The plot of pH versus absorbance obtained from the UV-vis spectra. In all cases, the SB (Schiff Base, imine) and PSB (Protonated Schiff Base, iminium) peaks are highlighted.

M. Towards turning the steric interaction in the vicinity of C13-C14 double bond

Using the all-*trans* retinal-bound mutant structures as a guide, bulky residues were introduced in the vicinity of the C13-C14 double bond to introduce steric interactions. Inspired by bacteriorhodopsin, our first screening effort was centered on mutating L121 to aromatic residues to mimic the steric interactions of the natural protein's Trp 86, Figure S3. [10, 11] Leu121 is ~ 3.6 Å away from C13, making it a suitable candidate to fulfill this goal, Figure S4. Therefore, L121W, L121Y, and L121F were incorporated in the **M1** construct. **M1**-L121F did not lead to soluble expression, but **M1**-L121W and **M1**-L121Y were solubly expressed and purified. The all-*trans* retinal-bound crystal structures of **M1**-L121W and L121Y were determined but attempts at crystallizing the 13-*cis* bound variants were unsuccessful. The overlay of all-*trans* retinal-bound **M1**-L121W and **M1** showed that the chromophore had rotated about its C14-C15 and C6-C7 torsion angles such that the polyene methyl groups point in the opposite direction from those of all-*trans* retinal-bound **M1**, with a concomitant translation in the direction approximately perpendicular to the polyene axis (Figure S5). **M1**-L121Y revealed some changes in retinal trajectory along the polyene but poor electron density for the β-ionone ring, indicating some disorder of the retinal inside the binding pocket. The failure in crystallizing 13-*cis*-bound proteins and the all-*trans* retinal chromophore disorder in these variants lead to the supposition that aromatic residues at position 121 may be too large to comfortably accommodate retinal.

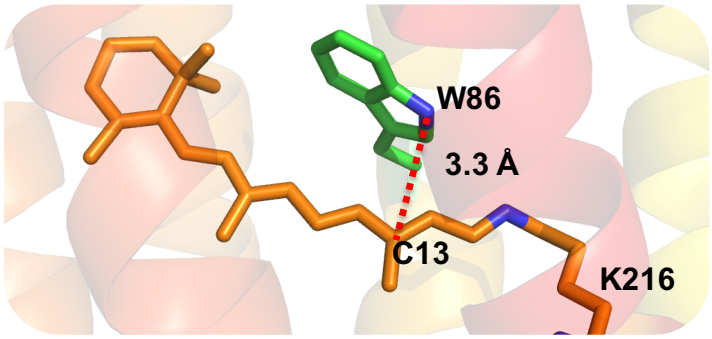

Figure S3. The binding pocket of bacteriorhodopsin, where W86 is located in the vicinity of C13-C14.

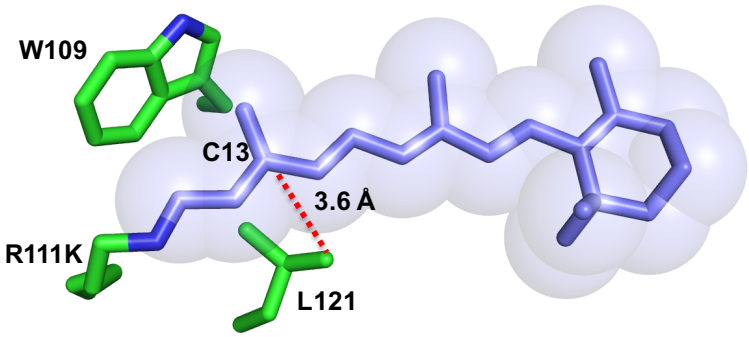

Figure S4. The CRABPII binding pocket. The L121 position is analogous to the W86 position in bacteriorhodopsin relative to retinal.

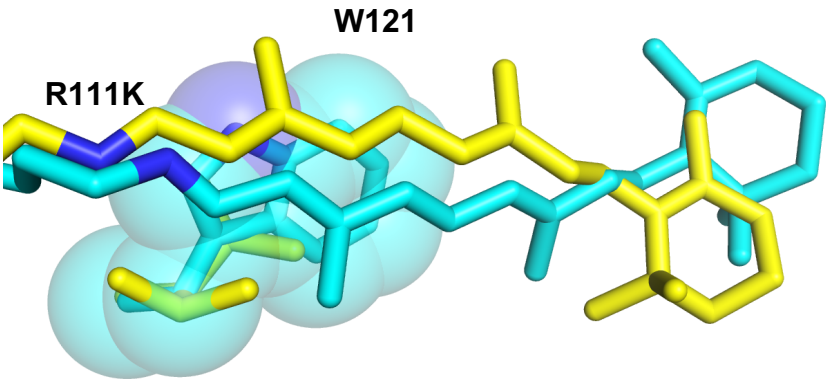

Figure S5. Overlay of **M1** (yellow) and **M1**-L121W (cyan). Introduction of a Trp at position 121 impinges on the bound chromophore, leading to a concomitant change in its trajectory.

N. HPLC extraction

i. Extraction and analysis of protein-bound retinals by using mercury lamp as an irradiation source

A solution of 50 μM protein with 25 μM all-*trans* retinal was prepared in PBS solution. After the indicated irradiation (described in **I**), the samples were flash frozen in liquid nitrogen. The samples were defrosted on ice. The retinylidene was hydrolyzed by acid (saturated citric acid was used by dropping the pH to 4.0). The protein:retinal solutions were denatured by adding equal volumes of ethanol to each sample and then the final solution was extracted with 200 μL hexane by vortexing and centrifugation at maximum speed for 1 min. The organic layer was transferred to an Eppendorf tube (1.5 mL), dried with sodium sulfate, and then concentrated to dryness under a nitrogen stream. Hexane extraction was performed to maximize recovery. The extracted samples were dissolved in hexane/ethyl acetate (90:10, 200 μL),.The resulting solution was analyzed by normal-phase HPLC (silica column, Zorbax Rx-SIL, 9.4 mm×25cm). The sample was eluted with hexane/ethyl acetate (90:10) at 3 ml/min. The products were detected at 363 nm.

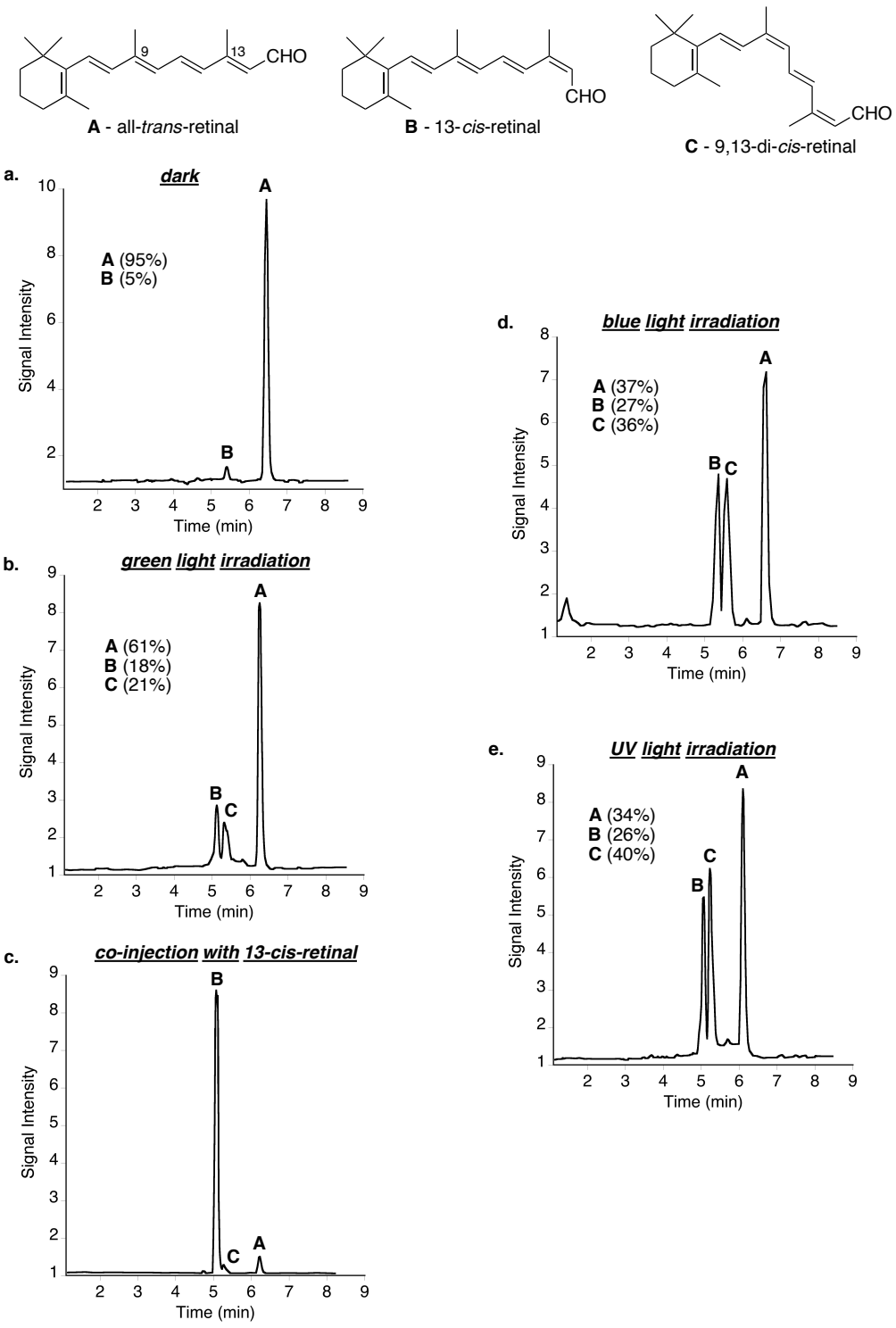

Figure S6. HPLC chromatogram of retinal isomers extracted from all-*trans* retinal bound **M1**-L121E: dark, after irradiation with mercury lamp- UV band pass filter (300-400 nm); blue band-pass filter (440 nm ± 20 nm); long-pass filter (>500 nm).The ratios were corrected using the extinction coefficient of each isomer (all-*trans* 48,000 $M^{-1}cm^{-1}$, 13-*cis* 38,770 $M^{-1}cm^{-1}$, and 9,13-*dicis* retinal 32,380 $M^{-1}cm^{-1}$).

ii. ^{1}H-NMR analysis of retinal extracted from protein/retinal complex

^{1}H-NMR of samples extracted as described above were recorded in $CDCl_3$ on a 900 MHz NMR. The identity of the extracted retinal was determined by the chemical shift of the aldehydic proton, which appears at a unique chemical shift for each isomer[12, 13] The NMRs were also compared to authentic samples of all-*trans* and 13-*cis* retinal.

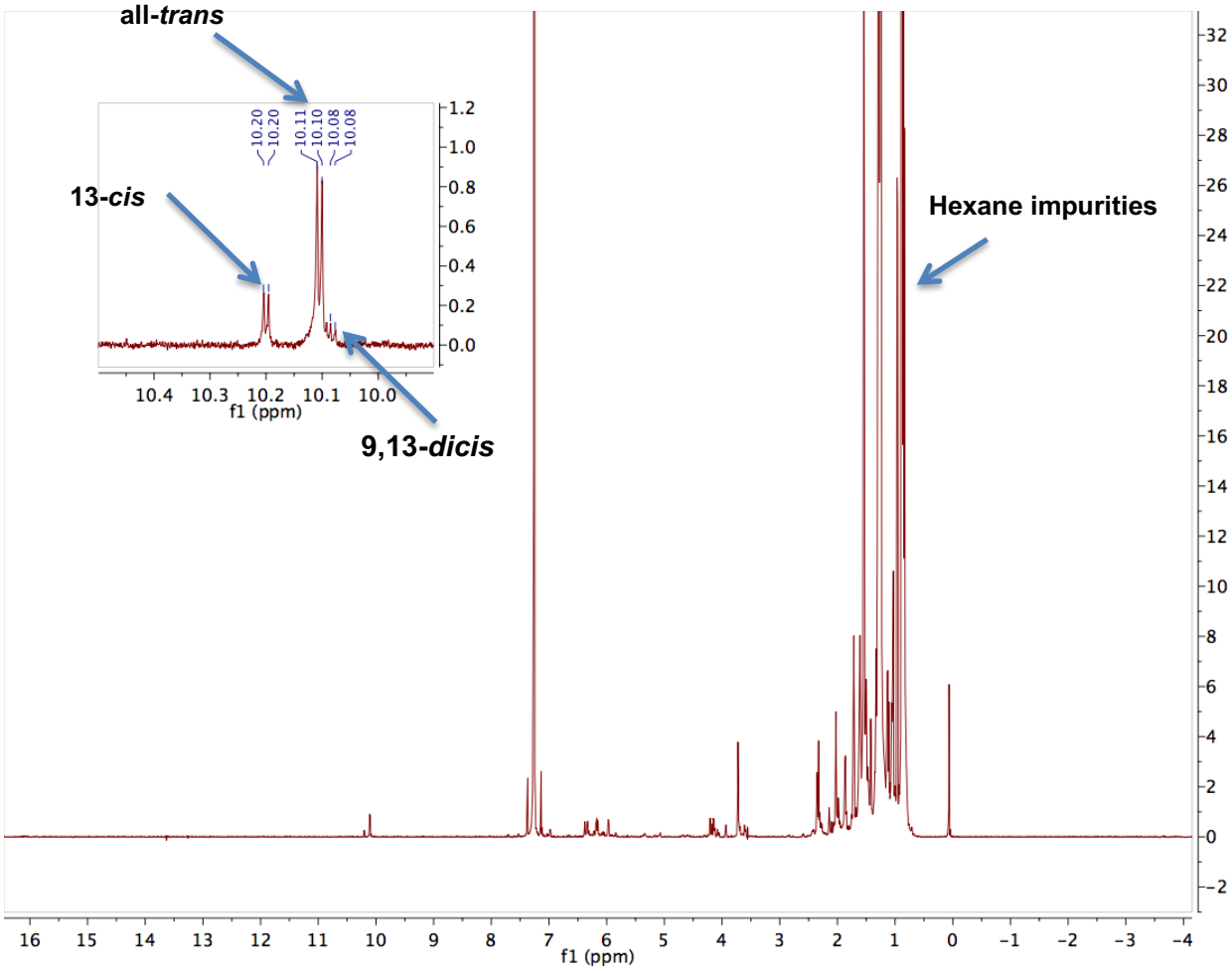

Figure S7. The ^{1}H-NMR spectra of retinal extracted from protein/retinal complex.

iii. Extraction and analysis of protein-bound retinal by using laser as an irradiation source

The same protocol as mentioned in **N-i** was used except that the same 399 nm laser used for the crystal irradiation experiments was used as an irradiation source (described in **O**). The solution was homogenized during irradiation by pipetting up and down. The extraction revealed the presence of 13-*cis* and 9,13-*dicis* retinal after 30 seconds and 5 minutes of irradiation of all-*trans* retinal bound **M1**-L121E samples.

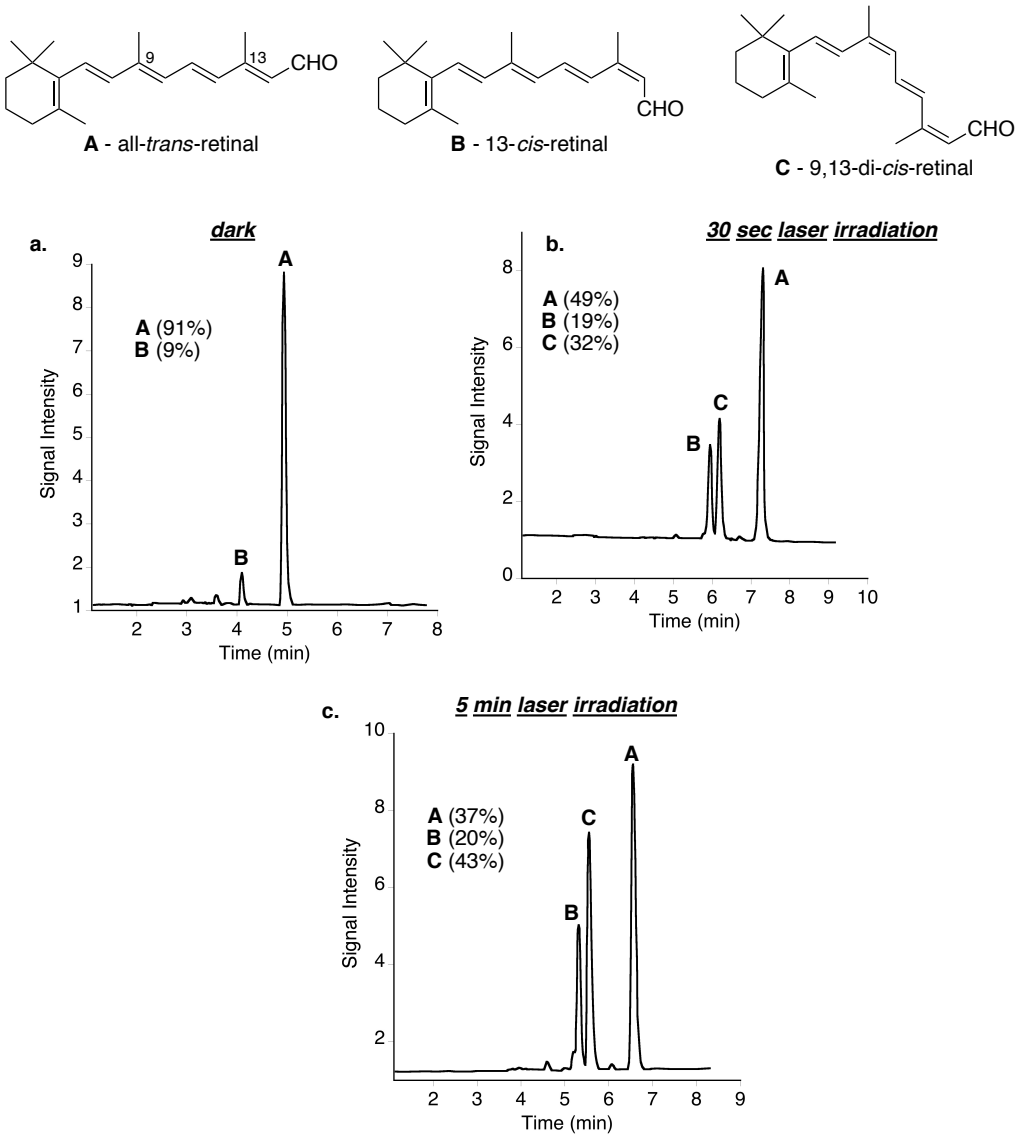

Figure S8. The HPLC chromatogram of **M1**-L121E bound with all-*trans* retinal: before irradiation, after 30 sec laser irradiation, after 5 min laser irradiation. The ratios were corrected using the extinction coefficient of each isomer (All-*trans* 48,000 $M^{-1}cm^{-1}$, 13-*cis* 38,770 $M^{-1}cm^{-1}$, and 9,13-*dicis* retinal 32,380 $M^{-1}cm^{-1}$).

O. Laser irradiation of crystals

A regenerative amplified Ti:Sapphire laser was used to produce femtosecond pulses centered at 798 nm with a bandwidth that corresponds to 40 fs when Transform-Limited (TL). The laser repetition rate was 1 kHz. The pulses were compressed after the amplifier using a pulse shaper (MIIPS-HD) utilizing the multiphoton intrapulse interference phase scan method. The TL pulses were used to generate the second harmonic signal (SHG) using a BBO crystal. The SHG pulses are centered at 399 nm (Figure S10) with a FWHM of 7.5 nm corresponding to 30 fs. The pulse energy was attenuated to about 1 µJ with an effective diameter of 3 mm, which were used to irradiate the crystals placed on the coverslips containing 4 µL of cryogenic buffer (pH=6.5) at different time periods. For green light irradiation, the samples were irradiated using the output of a frequency doubled Q-switched Nd:YAG laser operating at 532 nm (Mellennia, Spectra-Physics). The output was attenuated to around 200 mW and was sent unfocused with a beam diameter around 2.5 mm ($1/e^2$) at the crystals location.

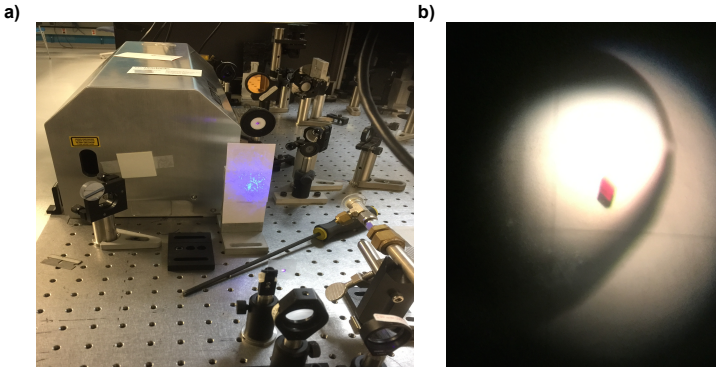

Figure S9. Irradiation of crystals. a) apparatus used to irradiate all-*trans*-bound **M1**-L121E crystals. b) The crystal used for irradiation study.

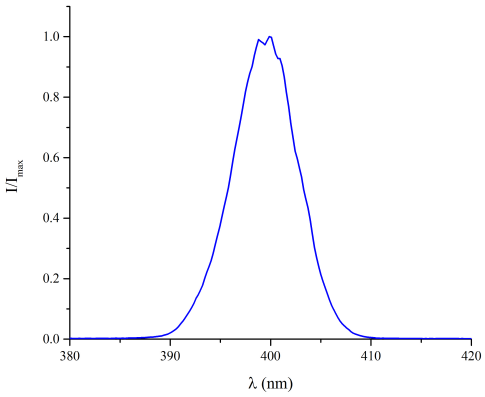

Figure S10. The spectrum of SHG centered at 399 nm.

P. Irradiation of M1-L121E/retinal crystals

To find the shortest exposure time that can lead to 13-*cis* formation in the crystal, the crystal was irradiated with the indicated 399 nm laser (as mentioned earlier) for 30 seconds and then the crystals were immediately flash frozen in liquid N_2. The 13-*cis* generated after 30 seconds of laser irradiation depicted the same β-ionone ring rotation as observed for 5 minutes of laser irradiated crystal (**M1**-L121E light state), Figure S11. While the overlay of this structure with all-*trans* retinal bound structure of **M1**-L121E (dark state) shows drastic differences in retinal trajectory and β-ionone ring.

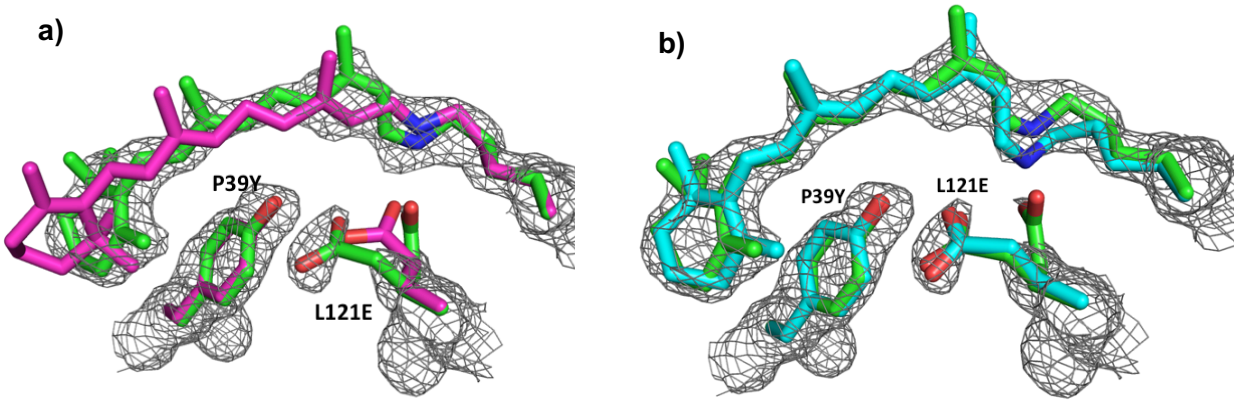

Figure S11. a) Overlay of the dark state **M1**-L121E (pink) and after 30 sec laser irradiation (green-13-*cis*) revealing the changes in the polyene and ionone ring conformation of retinal after laser irradiation. Electron density belongs to the crystal irradiated for 30 sec (countered at 1σ). b) Overlay of 30 sec irradiation structure (green) with five minutes' irradiation with laser (cyan) of **M1**-L121E demonstrating the similar ionone ring and polyene conformation verifying the formation of 13-*cis* after 30 sec laser irradiation. Electron density belongs to the crystal irradiated for 30 sec (countered at 1σ).

Q. Irradiation study of M1-L121E:P39Q/retinal complex

To investigate the role of the P39Y mutation in a selective isomerization of the C13-C14 double bond, this residue was mutated to Gln. The crystal structure of this mutant was obtained in the dark at 2.2 Å resolution. As shown in the overlay of **M1**-L121E:P39Q (dark state) vs. **M1**-L121E (dark state) replacing Tyr39 with Gln, significantly reduces steric interaction in the vicinity of the chromophore around the C13-C14 double bond. Furthermore, the chromophore is not pushed to the retinal trajectory as seen for **M1**-L121E, a conformation that is presumably necessary for retinal isomerization around C13-C14 double bond (Figure S12). Additionally, the UV spectrum, Figure S13a of **M1**-L121E:P39Q in contrast to **M1**-L121E, showed the PSB absorption (457nm) is red shifted to a new PSB absorbing at 507 nm upon irradiation with UV (B.P 300-400 nm). Interestingly, irradiation with green light retrieves the original PSB (457 nm). The irradiation of the **M1**-L121E:P39Q crystal with UV showed the drastic change in the color, presumably correlating with the shift observed in the UV-vis spectrum (Figure S13b). The crystal structure after irradiation was determined at 2.6 Å resolution. The conformation of polyene and β-ionone ring confirmed the presence of all-*trans* retinal after 5 minutes UV irradiation (Figure S13c). Furthermore, as shown in Figure S13d, the overlay of UV irradiated structure with **M1**-L121E bound with 13-*cis* generated after 5 minutes laser irradiation, further confirmed that the product of **M1**-L121E:P39Q irradiation is all-*trans* (It is not correlated with the 13-*cis* retinal trajectory). This mutation further proves the specific role of the P39Y mutation to pack against the chromophore and direct the isomerization around the C13-C14 double bond.

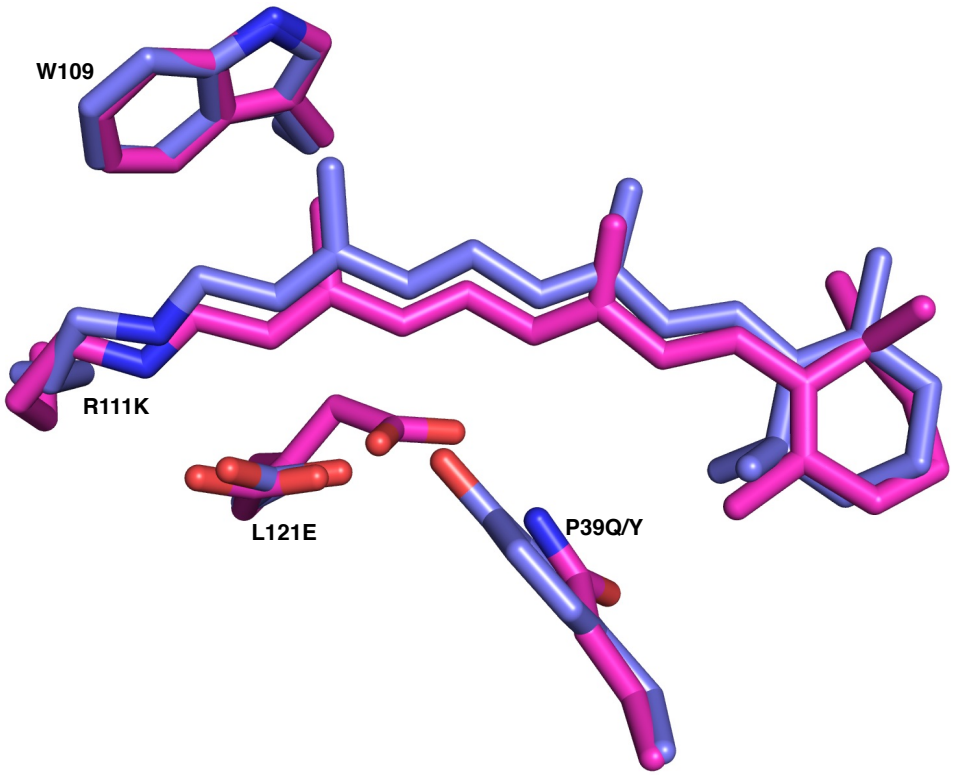

Figure S12. The overlay of **M1**-L121E (purple blue) with **M1**-L121E:P39Q (pink). P39Q mutation does not increase the steric interaction in the vicinity of C13-C14 double bond. Furthermore, in the absence of P39Y, the chromophore does not move to a trajectory seen for **M1**-L121E, highlighting the essential role of P39Y for defining the chromophore trajectory in **M1**-L121E and presumably directing the isomerization towards 13-*cis* isomer formation.

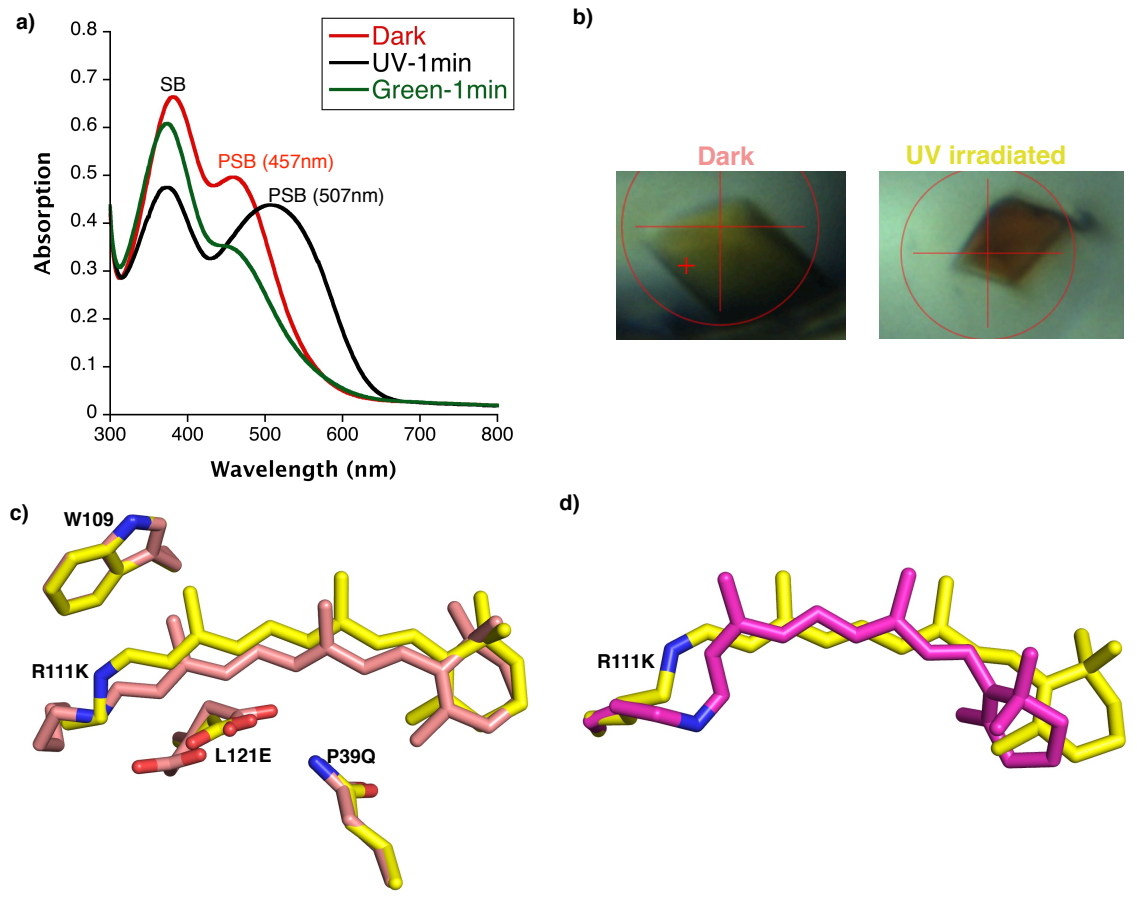

Figure S13. a) The UV-Vis. spectrum of **M1**-L121E:P39Q at dark, after UV (B.P.300-400 nm) irradiation, and after subsequent green light irradiation (L.P 500nm). b) The drastic color change in the crystal upon UV irradiation (the handheld UV lamp for TLC was used as a source of irradiation.). c) The overlay of dark state (pink), and UV irradiated (yellow) **M1**-L121E:P39Q crystal structures depicting the all-*trans* conformation for both states d) The overlay of UV irradiated **M1**-L121E:P39Q (yellow) vs. the light state of **M1**-L121E (magenta).

R. Thermal isomerization in M1-L121E/retinal crystal

To investigate the thermo-stability of 13-*cis* generated upon laser irradiation, after irradiation of crystals for 30 seconds, the crystals were left in the dark for 10 and 25 minutes and subsequently were flash frozen in liquid N_2. After data collection and data analysis, the electron density verifies the regeneration of all-*trans* retinal showing the thermo-isomerization of 13-*cis* to all-*trans* retinal in a single crystal. (Figure S14-S16)

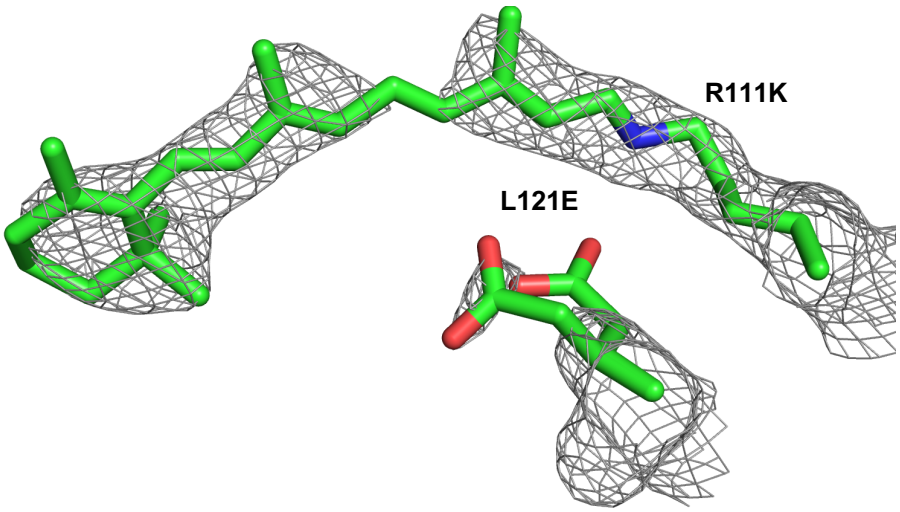

Figure S14. all-*trans* retinal-bound **M1**-L121E crystal after 30 sec irradiation with laser (399 nm) and subsequent incubation in the dark for 10 minutes (electron density contoured at 1σ). This crystal structure indicates the regeneration of all-*trans* retinal through the thermal isomerization of 13-*cis*. Although the chromophore adopted the all-*trans* retinal conformation, L121E does not reset completely to the initial dark state conformation.

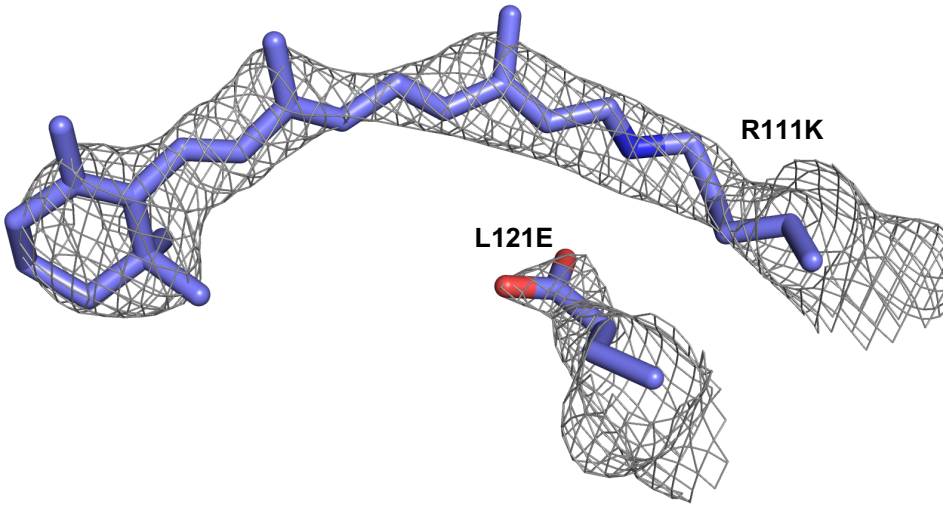

Figure S15. Structure from an all-*trans* retinal-bound **M1**-L121E crystal after 30 sec irradiation with laser (399 nm) and subsequent incubation in the dark for 25 minutes (electron density contoured at 1σ.) showing the regeneration of all-*trans* retinal and L121E adopted the same conformation as the initial dark state.

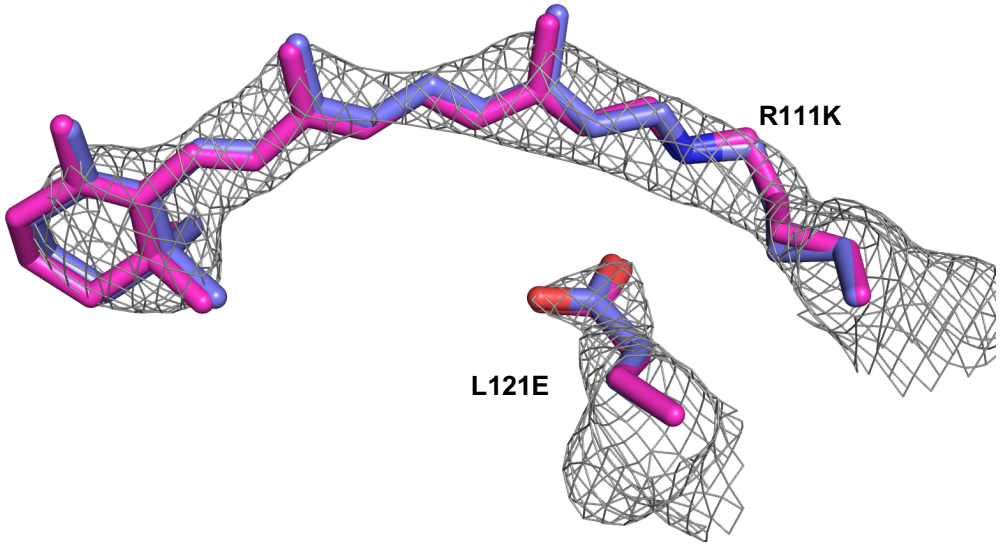

Figure S16. Overlay of structures from all-*trans* bound **M1**-L121E (dark state, pink) and after laser irradiation followed by incubation in the dark (25 minutes) (purple) verifying the structural similarity of the chromophore both before and after a complete photocycle. The electron density (contoured at 1σ) is calculated from the structure after 25 minutes incubation in the dark.

S. Overlay of 13-*cis* bound crystal structure at dark versus 13-*cis* generated after laser irradiation

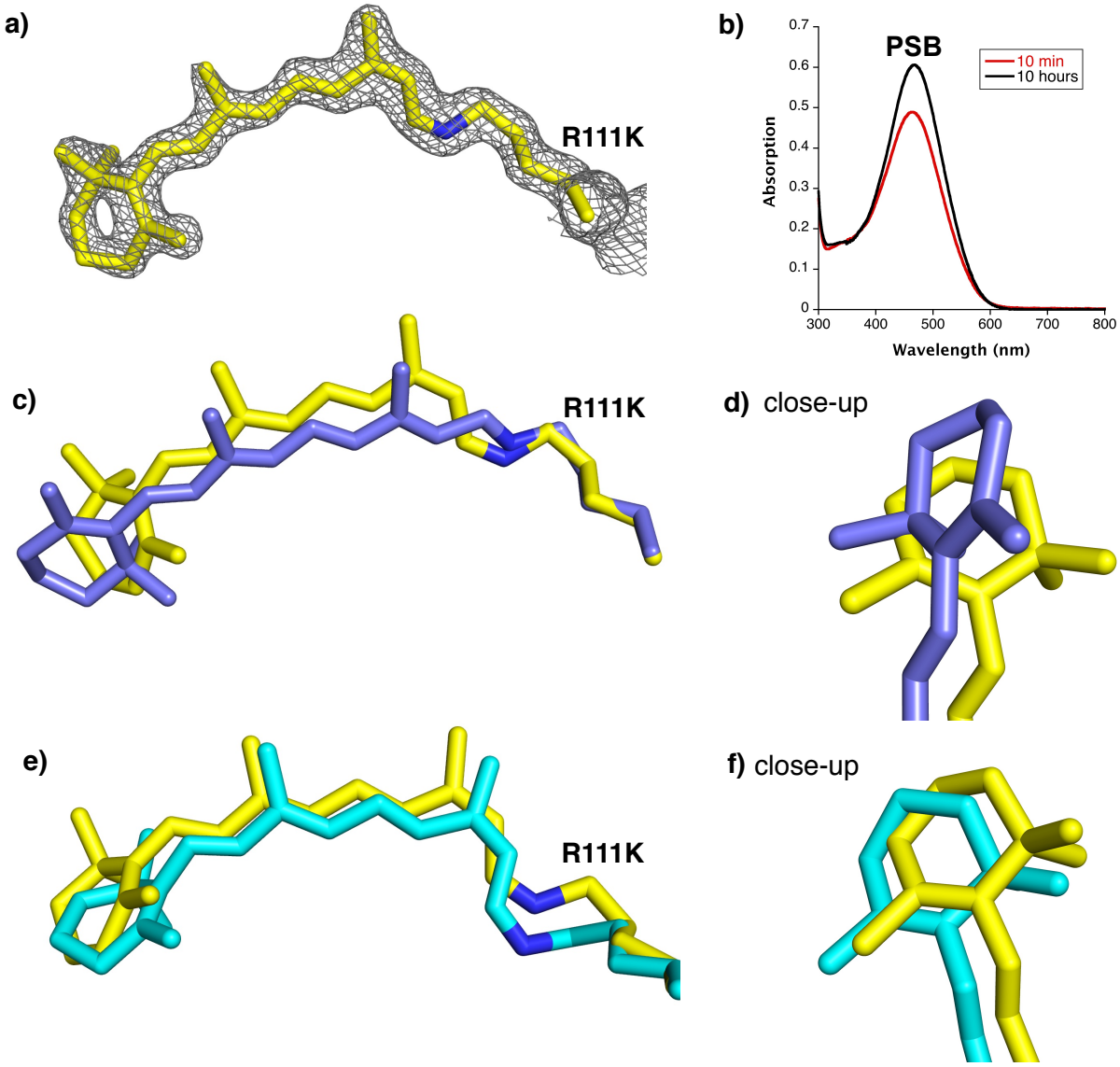

Figure S17. a) 13-*cis* electron density in **M1**-L121E:A32Y variant countered at 1.5σ. Atoms colored by type with C atoms yellow. b) The UV-vis. spectrum of **M1**-L121E:A32Y bound with the 13-*cis* retinal depicting the stable PSB after 10 hours of incubation. c) Overlay of 13-*cis* bound **M1**:L121E:A32Y (yellow) with all-*trans* bound **M1**:L121E (purple) without irradiation of either. d) A close-up view of the *β*-ionone ring trajectory in 13-*cis* bound **M1**-L121E-A32Y structure in dark (yellow) with all-*trans* dark state structure in **M1**-L121E (purple blue). e) Overlay of 13-*cis* retinal bound **M1**-L121E-A32Y (yellow) with the structure from a crystal of all-*trans* bound **M1**-L121E that was laser irradiated (5 min) and immediately frozen (cyan). f) Close-up view of the *β*-ionone ring trajectory in 13-*cis* bound **M1**-L121E:A32Y in dark (yellow) versus laser-irradiated (5 min and immediately frozen) all-*trans* bound **M1**-L121E.

T. Solution and crystal behavior of M1-L121Q/retinal complex

i. Irradiation study of M1-L121Q/retinal complex in solution

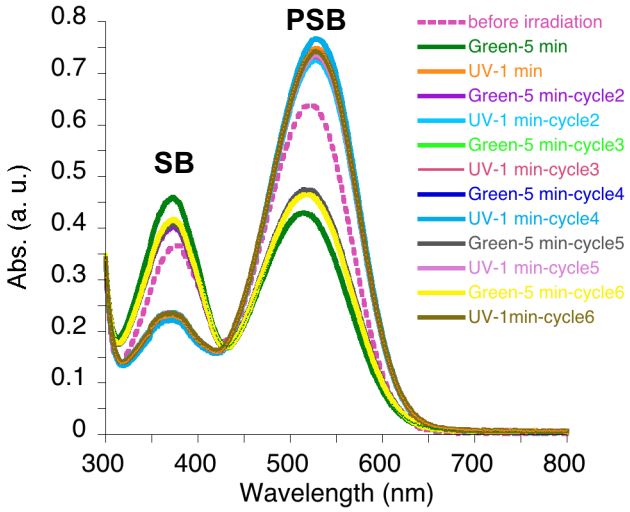

Figure S18. M1-L121Q bound with all-*trans* retinal photocycle by using mercury lamp as a source and UV band pass filter (300-400 nm) and long-pass filter (>500 nm).The SB (Schiff Base, Imine) and PSB (Protonated Schiff Base, iminium) peaks are highlighted.

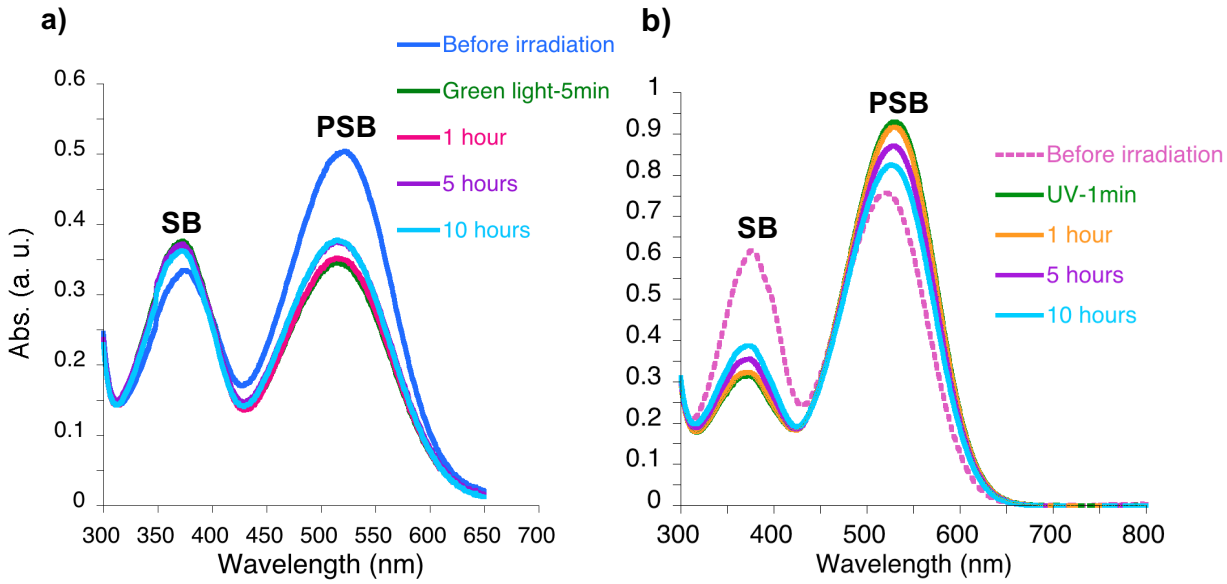

Figure S19. a) Green light irradiation (long-pass filter (>500 nm)) of **M1**-L121Q bound with all-*trans* for 5 min and monitoring the UV-vis spectra at different time intervals at dark. b) UV band-pass filter (300-400 nm) irradiation of **M1**-L121Q bound with all-*trans* for 1 min, and monitoring the UV-vis spectra at different time intervals at dark. The SB (Schiff Base, Imine) and PSB (Protonated Schiff Base, iminium) peaks are highlighted.

ii. pK_a determination of M1-L121Q/retinal complex

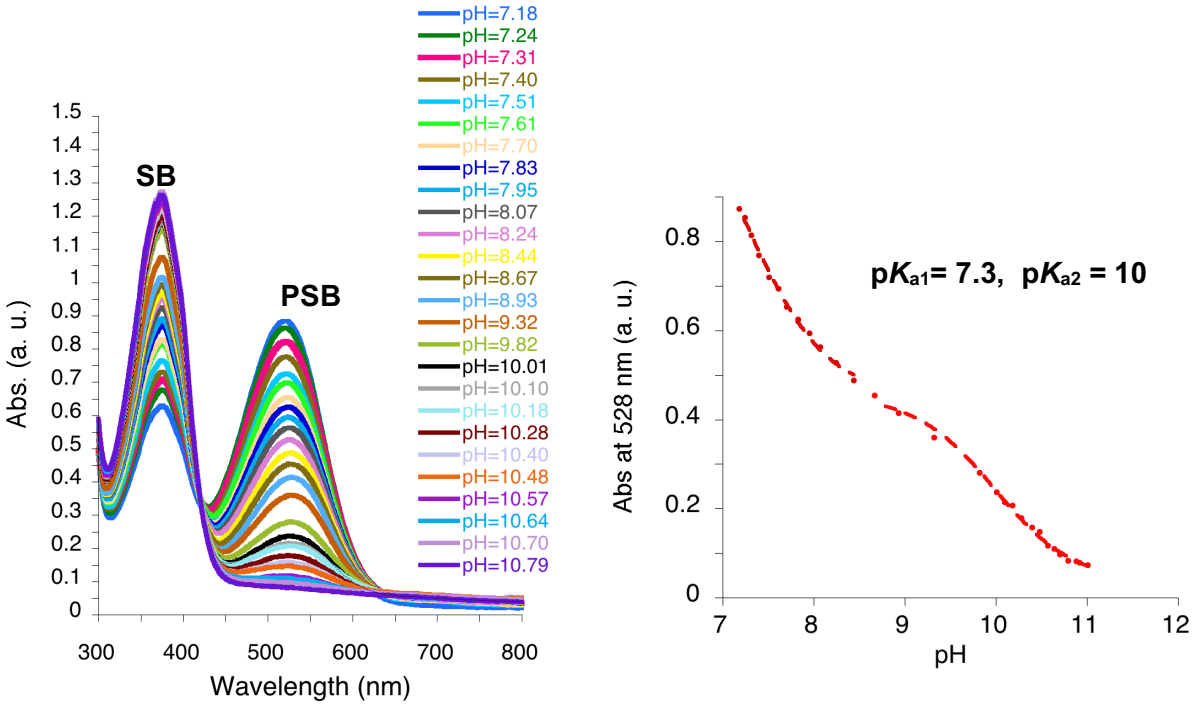

Figure S20. Base titration of **M1**-L121Q bound with all-*trans* retinal. Left pannel: UV-vis spectra; Right panel: The plot of pH versus absorbance obtained from the UV-vis spectra. In all cases, the SB (Schiff Base, Imine) and PSB (Protonated Schiff Base, iminium) peaks are highlighted.

iii. The Irradiation study of M1-L121Q/retinal crystals with laser

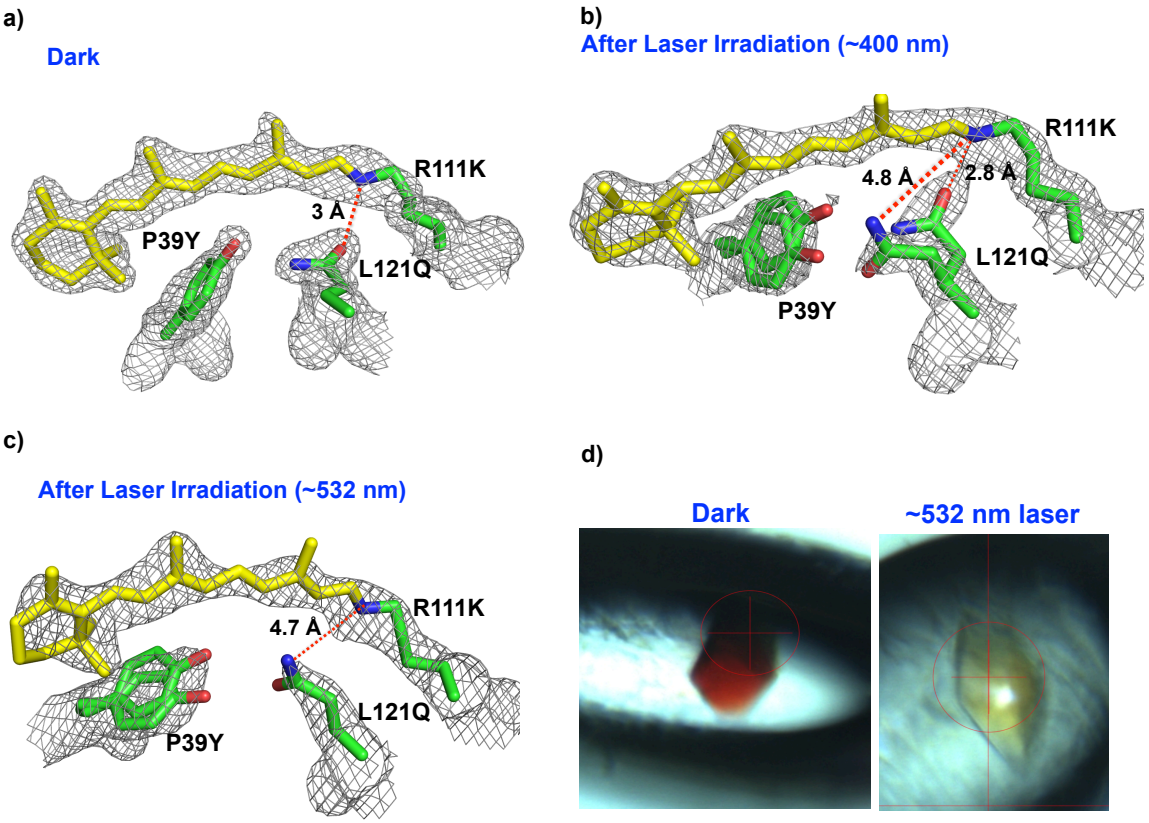

Figure S21. a) The crystal structure of **M1**-L121Q obtained in the dark. L121Q has a direct hydrogen bond with R111K. b) The crystal structure of **M1**-L121Q after 5 minutes irradiation with 399 nm laser. L121Q and P39Y adopt two distinct conformations but no isomerization occurs. L121Q in one conformation is far away from iminium (4.8 Å). c) After 10 min laser irradiation of crystals with 532 nm laser (close to protonated Schiff base maximum absorption) L121Q swings away from the iminium, lowering the pK_a of the protonated Schiff base, resulting in SB formation. d) A drastic color change of crystals upon irradiation with 532 nm laser.

U. X-ray Crystallography Tables

i. Table S3. The crystallography table for various dark and light states of all-*trans* bound **M1**-L121E.

	M1-L121E bound with all-*trans* retinal in dark	**M1-L121E bound with all-*trans* retinal, 5 minutes irradiation with 399 nm laser**	**M1-L121E bound with all-*trans* retinal, 30 seconds irradiation with 399 nm laser**	**M1-L121E bound with all-*trans* retinal, 30 seconds irradiation with 399 nm laser, 10 minutes incubation in dark**	**M1-L121E bound with all-*trans* retinal, 30 seconds irradiation with 399 nm laser, 25 minutes incubation in dark**
Space group	$P\,3_12_1$	$P\,3_12_1$	$P\,3_12_1$	$P\,3_12_1$	$P\,3_12_1$
a(Å)	58.986	58.567	58.343	58.586	58.501
b(Å)	58.986	58.567	58.343	58.586	58.501
c (Å)	100.314	98.974	99.865	100.178	99.982
α(°)	90	90	90	90	90
β(°)	90	90	90	90	90
δ(°)	120	120	120	120	120
Molecules per Asymmetric Unit	1	1	1	1	1
Total reflection	405325	503530	777250	478475	463610
Unique Reflection	16473 (1618)	12474 (1214)	16010 (1552)	12273 (1205)	13681(1345)
Completeness (%)	99.92 (100.00)	99.92 (99.92)	99.48 (98.66)	99.83 (100.00)	99.54 (99.78)
Average I/σ	34.4 (2.15)	26 (1.87)	35.5 (3.3)	36.75 (3.80)	44.63 (3.3)
R_{merge}	0.05 (0.87)	0.078 (0.95)	0.047 (0.36)	0.067 (0.68)	0.065 (0.62)
Resolution (Å) (Last Shell)	35.79 - 1.90 (1.93 - 1.90)	45.14 - 2.07 (2.14 - 2.07)	28.0 - 1.90 (1.97 - 1.90)	29.29 - 2.09 (2.16 - 2.09)	29.25 - 2.01 (2.01-2.08)
R_{work}/ R_{free}	19.50/22.74	19.31 /25.21	18.93/21.70	18.30/22.02	19.87/23.40
Bond Length (Å)	0.009	0.008	0.008	0.007	0.008
Bond Angle (°)	0.87	1.06	0.88	0.87	0.86
Average B factor	40.13	40.03	32.83	39.40	52.38
Number of water molecules	101	45	42	54	38
PDB ID	6MOP	6MQZ	6MQY	6MQW	6MQX

[a] Values in the parenthesis refer to the last resolution shell.

ii. Table S4. The crystallography table for 13-*cis* bound **M1**-L121E:A32Y, and all-*trans* bound **M1**-L121W, **M1**-L121Y, and **M1**-L121Q dark states.

	M1-L121E-A32Y bound with 13-*cis* retinal in dark	**M1-L121W bound with all-*trans* retinal in dark**	**M1-L121Y bound with all-*trans* retinal in dark**	**M1-L121Q bound with all-*trans* retinal in dark**
Space group	$P\,3_12_1$	$P\,3_12_1$	$P\,3_12_1$	$P\,3_12_1$
a(Å)	58.761	58.117	58.469	59.219
b(Å)	58.761	58.117	58.469	59.219
c (Å)	99.174	99.629	100.118	99.837
α(°)	90	90	90	90
β(°)	90	90	90	90
δ(°)	120	120	120	120
Molecules per Asymmetric Unit	1	1	1	1
Total reflection	556609	1093404	395603	552392
Unique Reflection	27796 (2743)	10327 (1019)	19270 (1890)	20945 (2022)
Completeness (%)	99.77 (100)	98.99 (98.25)	99.94 (99.89)	99.84 (98.92)
Average I/σ	36 (2.18)	22.8 (1.6)	39.9 (3.6)	45 (2.4)
R_{merge}	0.065 (0.60)	0.077 (0.58)	0.044 (0.51)	0.055 (0.87)
Resolution (Å) (Last Shell)	35.51 - 1.58 (1.64 - 1.58)	27.90 - 2.20 (2.28 - 2.20)	35.60 - 1.79 (1.85 - 1.79)	35.77 - 1.75 (1.81 -1.75)
R_{work}/ R_{free} (%)	20.29/22.18	22.62/26.57	22.31/24.72	21.47/23.34
Bond Length (Å)	0.006	0.009	0.007	0.009
Bond Angle (°)	0.86	1.04	0.95	0.92
Average B factor	32.72	56.32	30.86	32.99
Number of water molecules	111	29	99	67
PDB ID	6MPK	6MOQ	6MOR	6MOV

[a] Values in the parenthesis refer to the last resolution shell.

iii. Table S5. The crystallography table for different light states of all-*trans* bound **M1**-L121Q.

	M1-L121Q bound with all-*trans* retinal, 5 minutes irradiation with laser (399 nm)	**M1-L121Q- bound with all-*trans* retinal, 10 minutes irradiation with laser (532 nm)**
Space group	$P\,3_12_1$	$P\,3_12_1$
a(Å)	59.075	59.238
b(Å)	59.075	59.238
c (Å)	99.814	99.393
α(°)	90	90
β(°)	90	90
δ(°)	120	120
Molecules per Asymmetric Unit	1	1
Total reflection	378799	545064
Unique Reflection	17237 (1682)	11843 (1167)
Completeness (%)	99.94 (100.00)	99.82 (98.90)
Average I/σ	40.6 (2.55)	19.3 (1.8)
R_{merge}	0.044 (0.734)	0.06 (0.51)
Resolution (Å) (Last Shell)	35.72 - 1.87 (1.937 - 1.87)	35.69 - 2.12 (2.20 - 2.12)
R_{work}/ R_{free} (%)	21.52/25.96	18.85/24.31
Bond Length (Å)	0.009	0.009
Bond Angle (°)	0.95	0.94
Average B factor	35.95	41.35
Number of water Molecules	50	43
PDB ID	6MQI	6MQJ

[a] Values in the parenthesis refer to the last resolution shell.

iv. Table S6. The crystallography table for dark and light states of all-*trans* bound **M1**-L121E:P39Q.

	M1:L121E :P39Q bound with all-*trans* in dark	**M1:L121E :P39Q bound with all-*trans* 5 minutes UV irradiation**
Space group	$P\,3_12_1$	$P\,3_12_1$
a(Å)	58.546	58.476
b(Å)	58.546	58.476
c (Å)	99.525	99.552
α(°)	90	90
β(°)	90	90
δ(°)	120	120
Molecules per Asymmetric Unit	1	1
Total reflection	258241	534615
Unique Reflection	10769 (1059)	6064 (570)
Completeness (%)	99.94 (99.81)	99.59 (97.43)
Average I/σ	14.5 (2.2)	11.25 (2)
R_{merge}	0.089 (0.64)	0.15 (0.89)
Resolution (Å) (Last Shell)	45.18 - 2.18 (2.26 - 2.18)	33.18-2.65 (2.74 - 2.65)
R_{work}/ R_{free}	20.35/25.01	19.12/27.34
Bond Length (Å)	0.009	0.010
Bond Angle (°)	0.94	1.01
Average B factor	31.76	32.46
Number of water molecules	25	12
PDB ID	6MOX	6MR0

[a] Values in the parenthesis refer to the last resolution shell.

V. References

1. Nosrati, M.; Berbasova, T.; Vasileiou, C.; Borhan, B.; Geiger, J. H., A Photoisomerizing Rhodopsin Mimic Observed at Atomic Resolution. *Journal of the American Chemical Society* **2016,** *138* (28), 8802-8808.
2. Berbasova, T.; Nosrati, M.; Vasileiou, C.; Wang, W.; Lee, K. S. S.; Yapici, I.; Geiger, J. H.; Borhan, B., Rational Design of a Colorimetric pH Sensor from a Soluble Retinoic Acid Chaperone. *Journal of the American Chemical Society* **2013,** *135* (43), 16111-16119.
3. Maeda, T.; Van Hooser, J. P.; Driessen, C. A.; Filipek, S.; Janssen, J. J.; Palczewski, K., Evaluation of the role of the retinal G protein-coupled receptor (RGR) in the vertebrate retina in vivo. *Journal of neurochemistry* **2003,** *85* (4), 944-56.
4. Gill, S. C.; von Hippel, P. H., Calculation of protein extinction coefficients from amino acid sequence data. *Analytical biochemistry* **1989,** *182* (2), 319-26.
5. Berbasova, T.; Santos, E. M.; Nosrati, M.; Vasileiou, C.; Geiger, J. H.; Borhan, B., Light-Activated Reversible Imine Isomerization: Towards a Photochromic Protein Switch. *ChemBioChem* **2016,** *17* (5), 407-414.
6. Otwinowski, Z.; Minor, W., [20] Processing of X-ray diffraction data collected in oscillation mode. *Methods in Enzymology* **1997,** *276*, 307-326.
7. Murshudov, G. N.; Vagin, A. A.; Dodson, E. J., Refinement of Macromolecular Structures by the Maximum-Likelihood Method. *Acta Crystallographica Section D* **1997,** *53* (3), 240-255.
8. Adams, P. D.; Afonine, P. V.; Bunkoczi, G.; Chen, V. B.; Davis, I. W.; Echols, N.; Headd, J. J.; Hung, L.-W.; Kapral, G. J.; Grosse-Kunstleve, R. W.; McCoy, A. J.; Moriarty, N. W.; Oeffner, R.; Read, R. J.; Richardson, D. C.; Richardson, J. S.; Terwilliger, T. C.; Zwart, P. H., PHENIX: a comprehensive Python-based system for macromolecular structure solution. *Acta Crystallographica Section D* **2010,** *66* (2), 213-221.
9. Emsley, P.; Lohkamp, B.; Scott, W. G.; Cowtan, K., Features and development of Coot. *Acta Crystallographica Section D-Biological Crystallography* **2010,** *66*, 486-501.
10. Luecke, H.; Schobert, B.; Cartailler, J.-P.; Richter, H.-T.; Rosengarth, A.; Needleman, R.; Lanyi, J. K., Coupling photoisomerization of retinal to directional transport in bacteriorhodopsin, Edited by D. C. Rees. *Journal of Molecular Biology* **2000,** *300* (5), 1237-1255.
11. Ernst, O. P.; Lodowski, D. T.; Elstner, M.; Hegemann, P.; Brown, L. S.; Kandori, H., Microbial and Animal Rhodopsins: Structures, Functions, and Molecular Mechanisms. *Chemical Reviews* **2014,** *114* (1), 126-163.
12. Bolze, C. S.; Helbling, R. E.; Owen, R. L.; Pearson, A. R.; Pompidor, G.; Dworkowski, F.; Fuchs, M. R.; Furrer, J.; Golczak, M.; Palczewski, K.; Cascella, M.; Stocker, A., Human Cellular Retinaldehyde-Binding Protein Has Secondary Thermal 9-cis-Retinal Isomerase Activity. *Journal of the American Chemical Society* **2014,** *136* (1), 137-146.
13. Wang, K.-W.; Wang, S.-W.; Du, Q.-Z., Complete NMR assignment of retinal and its related compounds. *Magnetic Resonance in Chemistry* **2013,** *51* (7), 435-438.